Tricalcium Silicate Hydration Reaction in the Presence of Comb-Shaped Superplasticizers: Boundary Nucleation and Growth Model Applied to Polymer-Modified Pastes

ARTICLE *in* THE JOURNAL OF PHYSICAL CHEMISTRY C · MAY 2012

Impact Factor: 4.77 · DOI: 10.1021/jp209156n

THE JOURNAL OF PHYSICAL CHEMISTRY C

Article

pubs.acs.org/JPCC

Tricalcium Silicate Hydration Reaction in the Presence of Comb-Shaped Superplasticizers: Boundary Nucleation and Growth Model Applied to Polymer-Modified Pastes

Francesca Ridi,[†] Emiliano Fratini,[†] Paola Luciani,[†] Frank Winnefeld,[‡] and Piero Baglioni*[,†]

[†]Department of Chemistry and CSGI, University of Florence, via della Lastruccia 3-Sesto Fiorentino, I-50019 Florence, Italy

[‡]Empa, Swiss Federal Laboratories for Materials Science and Technology, Laboratory for Concrete and Construction Chemistry, Überlandstrasse 129, 8600 Dübendorf, Switzerland

Supporting Information

ABSTRACT: The Boundary Nucleation and Growth Model (BNGM), developed for the analysis of the hydration reaction of tricalcium silicate, has been applied to study the kinetic behavior of pastes containing chemical admixtures. Four comb-shaped polycarboxylate ether (PCE) superplasticizers with well-known molecular structures have been added to tricalcium silicate. The BNGM analysis performed on this series of additives allows insights into the effect of the molecular architecture of the PCEs on the induction time and rate constants. The results show that decreasing the length of the polyethylene oxide side chains of the PCE molecules increases the induction time. Also, the side chain density, which highly influences the adsorption of the polymer to the C_3S unreacted grains, is shown to significantly affect the duration of the induction period: in particular, molecules with low side chain density delay the setting of the paste to a greater extent than molecules with denser side chains. Moreover, the chemical admixtures influence the rate constants of the nucleation and growth processes, both reducing them and affecting their temperature dependence.

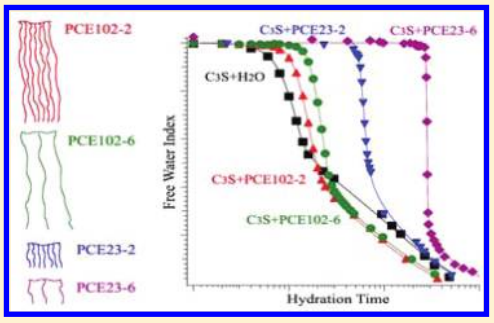

INTRODUCTION

The comprehension of the fundamental mechanisms underlining the hydration reaction of a cement powder is still a focal point in cement chemistry research. In particular, two main steps characterize the conversion of the dry powder to the final hydrated products: a nucleation and growth period, which is followed by a diffusion-limited hydration stage.[1] The physicochemical comprehension of these kinetic processes is important to understand the mechanisms by which hydrated products (mainly hydrated calcium silicate, C−S−H) form, to control and design the C−S−H with "ad-hoc" properties, especially through the use of additives.

The BNGM was applied for the first time to the analysis of the tricalcium silicate (C_3S) hydration reaction by Thomas.[2] This mathematical description of the hydrates formation is a substantial improvement over the Avrami−Erove'ev (A−E) equation. The BNGM was implemented as a generalization of the A−E equation to fully comply with the fact that the nucleation of new phases mainly occurs at the boundary interface of the C_3S grains. It was shown to provide a very good physicochemical description of the early hydration of tricalcium silicate as followed by isothermal calorimetry (IC),[2,3] quasi-elastic neutron scattering (QENS),[4] and differential scanning calorimetry (DSC).[5] Moreover, the BNGM does not need an explicit parameter for the induction time (the initial period where the evolved heat is almost zero), as required by the classical A−E treatment, confirming that this threshold is not linked to a separate chemical process, but only to the fact that at the first stage of the reaction the global rate is low because only a negligible number of nuclei are forming or growing. In the absence of chemical retarders, a true induction is not believed to occur for C_3S hydration.[1]

In a subsequent publication, the BNGM[3] was modified by the introduction of a t_0 parameter, a time constant that shifts the beginning of the nucleation and growth process from the time of mixing. This "modified BNGM" (or "generalized BNGM") can be applied to all of those systems where a real induction period is present, as pastes in which some retarding admixture is added to. In these last mentioned cases, the BNGM cannot adequately reproduce the experimental data without the introduction of the t_0.

It is worth stressing that, if the generalized version of the model is applied to a neat C_3S paste, t_0 results null or takes even negative values. In particular, t_0 is zero if there are no nuclei present at the time of mixing and if the nucleation begins at a constant linear growth rate, while negative values are associated with the presence of nuclei already at the time of mixing and/or with a faster nucleation rate at the beginning of the reaction. Consequently, t_0 will be positive when nucleation is inhibited by the presence of a chemical retarder (a true

Received: September 22, 2011
Revised: April 26, 2012
Published: April 30, 2012

induction period) or if the nucleation rate is slower at the beginning of the reaction.[3]

Important contributions reported on the influence of inorganic additions to tricalcium silicate hydration have been made. In particular, Thomas et al. studied the effect of nucleation seeding,[6] showing that C−S−H seeds cause hydration products to form within the pore space between the C_3S grains, thus accelerating the process. In another paper, the hydration of C_3S in the presence of $CaCl_2$, a widely used accelerator, is investigated by means of isothermal calorimetry and SANS measurements.[3] By applying the modified BNGM to the calorimetric data, Thomas and co-workers showed that $CaCl_2$ increases the early hydration rate and the total amount of early hydration by increasing the rate of nucleation of new products on the grains surface, while leaving the growth rate almost unaffected.

The study of the hydration reaction of pastes modified with chemical admixtures is still an unexplored field, mainly because the retardation effect induced by these additives is often too strong to allow the acquisition of the whole kinetic curve by means of IC, that is, the standard technique applied by cement industries for the study of the exothermic reaction of the cement with water. Some other techniques make it possible to monitor the hydration of chemically modified pastes, such as near-infrared spectroscopy,[7] QENS,[8−12] or DSC.[13−15] In particular, a very recent work[5] shows that a very good agreement exists between the nucleation and growth constant rates obtained by BNGM fittings of the C_3S hydration kinetics as followed by means of DSC and IC. The great advantage of the DSC method with respect to IC is the possibility to monitor very long processes such as those reported in the presence of superplasticizers, without the continuous use of the calorimeter and without any significant loss in the instrumental sensitivity.

For several decades, the addition of superplasticizers to the fresh mixture has been the best-established method to enhance the workability and placement characteristics of concrete. The most recent superplasticizers belong to the polycarboxylic ether (PCE) family. In the simplest case, they consist of a polyacrylic or polymethacrylic backbone with grafted polyethylene oxide side chains. PCE superplasticizers do not only change rheology, but also influence the kinetics of cement hydration. Both of these effects depend on the PCEs' ability to adsorb on the surface of the cement particles. In particular, polymers mainly adsorb onto the aluminate and ferrate phases and their hydration products.[16] Nevertheless, a significant amount also adsorbs onto both anhydrous and hydrated silicate phases.[16,17] It is commonly recognized that the impact on rheology is mostly related to the early tricalcium aluminate hydration,[16−22] while the retarding effect of PCE refers to their interaction with the C_3S hydration process.[14,22,23] Previous studies on the adsorption propensity of PCE with controlled molecular structure on cement and on synthetic silicate and aluminate phases showed that the parameter mostly affecting the adsorption is the charge density of the polymers.[20,23−27] In particular, the adsorption increases as the side chain's density of the polymers decreases (a higher number of negative charges due to the unsubstituted carboxylic groups is present on the backbone) and as the side chain length decreases (the accessibility to the negative charges on the backbone is not limited by steric hindrance). The retarding effect of PCEs on the hydration kinetics varies according to the adsorption:[20,23] lower grafting densities and shorter side chains lead to higher charged polymers, and thus promote their adsorption on the solid phases, through the complexing effect of the calcium ions.[21]

The main aim of this work is the validation of the generalized BNGM for the quantitative description of the nucleation and growth processes in hydrating C_3S pastes containing PCE superplasticizers. Four different comb-shaped PCE polymers with controlled molecular structure have been considered for this study. The kinetic curves were followed by DSC at four different temperatures, starting from the mixing time until the unreacted water was less than 5%, which is very close to the end of the diffusional period. The influence of the structural architecture (i.e., grafting density and side chain length) on the C_3S hydration process is evaluated with respect to the change in the initial induction period and the rate constants. The effects of PCEs on the activation energy of the nucleation and growth processes are also critically reviewed along with the extracted diffusional constants.

MATERIALS AND METHODS

Pure triclinic tricalcium silicate was obtained from CTG-Italcementi (Bergamo, Italy). The BET specific surface area is 0.65 m^2/g, and the mean radius of the grains is 4.66 μm. Four comb-shaped polycarboxylate-type polymers (PCE) have been used for this study. Polyethylenglycol side chains are grafted on methacrylic acid backbones (chemical structure sketched in Figure 1). The characteristics of the selected polymers are described in Table 1.

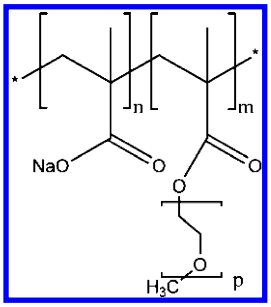

Figure 1. Chemical structure of the investigated PCEs with controlled density (n:m) and length (p) of the side chains.

Table 1. Characteristics of the Polycarboxylate-type Superplasticizers

	length of side chain (p)	density of side chains (n:m)	M_N[a] (g/mol)	M_W[b] (g/mol)	PDI[c]
PCE102-2	102	2:1	16 800	78 000	4.7
PCE102-6	102	6:1	14 600	67 000	4.6
PCE23-2	23	2:1	8700	25 600	2.9
PCE23-6	23	6:1	7600	18 900	2.5

[a]M_N: Number average molecular weight. [b]M_W: Mass average molecular weight. [c]PDI = M_W/M_N: polydispersity index.

Samples for DSC measurements were prepared with a 0.4 water/solid ratio by mass. 50 mg of C_3S was manually mixed with 20 mg of 10 g/L superplasticizer solutions (water purified by a Millipore Organex system; $R \geq 18$ MW cm). Roughly 40 mg of this paste was transferred in a steel pan (diameter 7.4 mm, capacity 60 μL) and sealed with the appropriate cover, equipped with an O-ring to avoid water leaking. The steel pans containing the samples were maintained in a thermostatic bath at constant temperatures (10, 20, 30, and 40 °C ± 0.1 °C).

dx.doi.org/10.1021/jp209156n | J. Phys. Chem. C 2012, 116, 10887−10895

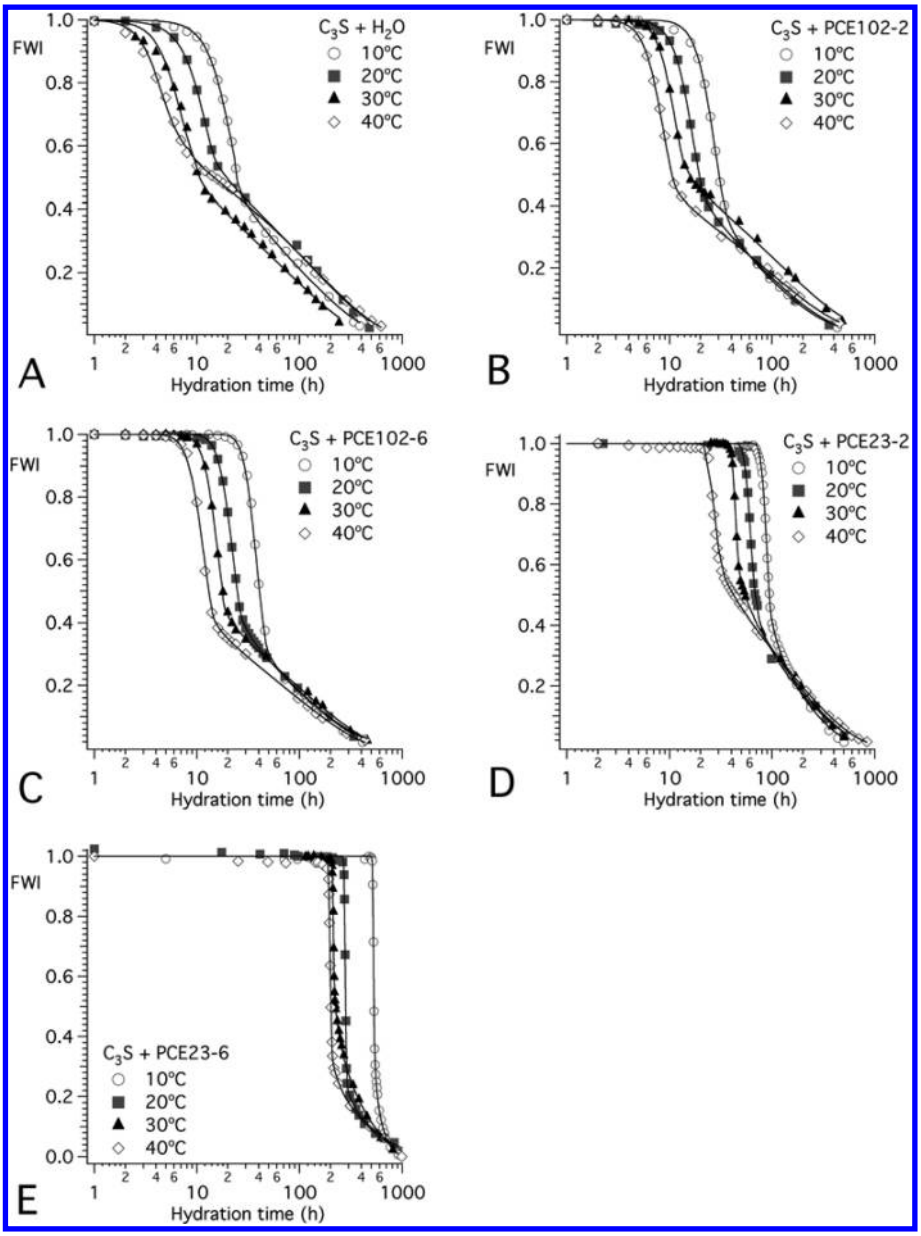

Figure 2. Hydration kinetics of C_3S (A) in pure water, (B) with PCE102-2, (C) with PCE102-6, (D) with PCE23-2, and (E) with PCE23-6. The generalized BNGM fittings combined with diffusion-limited model are reported on each data set as continuous lines.

Periodically, the samples were removed from the thermostatic bath and analyzed with the calorimeter. Differential scanning calorimetry measurements were performed using a DSC Q2000 (TA Instruments, Milan). The measurements were carried out with the following temperature program: equilibrate to −30 °C, isothermal for 1 min, from −30 to −12 °C at 20 °C/min, from −12 to +35 °C at 4 °C/min. Two different samples have been monitored throughout the curing period for each admixture and temperature.

Generalized Boundary Nucleation and Growth Model. The BNGM was first developed to describe metal phases transformations by J. Cahn.[28] When applied to a diphasic system undergoing a sol−gel transition, as in the case of C_3S hydration reaction, it is worth noting that the model is phenomenological. Nevertheless, the mathematical derivation obtained by Thomas for this system convincingly supplies Cahn's formalism with the physical meaning to describe the nucleation and growth processes in hydrating C_3S.

According to the modified BNGM, the volume fraction of transformed phase originating from nuclei on the same grain boundary, X, can be expressed by:

$$X = 1 - \exp[-2O_V^B \int_0^{G(t-t_0)} (1 - \exp(-Y^e))dy] \quad (1)$$

where O_V^B is the total area of the grain boundaries (randomly distributed in the original untransformed volume) per unit volume; G is the linear growth rate; t_0 represents the effective induction time introduced by the presence of the PCE polyelectrolyte; t is the time after the mixing; y is the distance from the transforming boundary (i.e., Gt); and Y^e is the extended area fraction of the intersection between a plane at distance y from the boundary and all regions nucleated on the grain boundary. Y^e can be mathematically described by:

dx.doi.org/10.1021/jp209156n | J. Phys. Chem. C 2012, 116, 10887−10895

Table 2. Fitting Parameters Obtained with the Generalized Boundary Nucleation and Growth Model Combined with the Diffusion-Limited Model[a]

T (°C)	t_0 (h)	t_d (h)	Δt_{BNG}[b] (h)	FWI_d	k_B (h^{-1})	k_G (h^{-1})	k_B/k_G	$D \times 10^{-15}$ (m^2 h^{-1})
H_2O								
10	−2.1(4)	24(1)	26(1)	0.21(2)	0.0437(2)	0.042(2)	1.04(5)	6.2(6)
20	−1.95(7)	14(1)	16(1)	0.22(2)	0.0720(5)	0.07(2)	1.0(3)	5.6(3)
30	−0.7(5)	10(1)	11(1)	0.35(3)	0.135(5)	0.127(3)	1.08(6)	8.7(8)
40	−0.2(1)	8(1)	8(1)	0.47(5)	0.218(7)	0.18(3)	1.2(2)	5.4(3)
PCE102-2								
10	2(1)	34(1)	32(2)	0.12(1)	0.0411(3)	0.052(4)	0.79(7)	7.4(7)
20	1.721(3)	20(1)	18(1)	0.25(2)	0.0642(2)	0.0929(9)	0.69(1)	7.7(4)
30	1.9(2)	14(1)	12(1)	0.39(4)	0.1126(5)	0.16(2)	0.70(9)	5.3(2)
40	0.68(4)	11(1)	10(1)	0.37(4)	0.131(1)	0.234(2)	0.55(1)	6.1(2)
PCE102-6								
10	14(4)	46(1)	32(5)	0.14(1)	0.0415(4)	0.055(5)	0.75(7)	4.6(8)
20	6.3(1)	26(1)	20(1)	0.20(2)	0.0624(4)	0.090(3)	0.69(3)	6.4(2)
30	4.5(1)	18(1)	13(1)	0.23(2)	0.0885(9)	0.13(1)	0.68(6)	5.6(2)
40	2 (1)	14(1)	12(2)	0.25(2)	0.113(4)	0.18(2)	0.63(9)	6.5(4)
PCE23-2								
10	61.8(2)	94(1)	32(1)	0.22(2)	0.036(1)	0.054(4)	0.67(7)	6.8(4)
20	41.7(3)	70(1)	28(1)	0.32(3)	0.050(1)	0.065(1)	0.77(3)	4.8(5)
30	34.5(6)	47(1)	12(2)	0.32(3)	0.096(2)	0.10(3)	0.9(3)	5.8(2)
40	19.0(1)	30(1)	11(1)	0.46(5)	0.1254(6)	0.129(2)	0.97(2)	5.3(1)
PCE23-6								
10	496(1)	538(1)	42(2)	0.24(2)	0.0358(5)	0.06(1)	0.59(9)	8.6(5)
20	263.0(4)	286(1)	23(1)	0.14(1)	0.060(2)	0.109(2)	0.55(3)	1.8(2)
30	201.5(3)	219(1)	17(1)	0.36(4)	0.0749(3)	0.09(2)	0.8(2)	4.9(3)
40	182.8(3)	207(1)	25(1)	0.20(2)	0.0636(9)	0.060(2)	1.06(5)	2.7(5)

[a]In parentheses are the standard deviations in least significant digits. [b]Δt_{BNG}: Duration of the nucleation and growth period, defined as $t_d - t_0$.

$$Y^e = \frac{\pi I_B}{3} G^2 (t - t_0)^3 \left[1 - \frac{3y^2}{G^2(t - t_0)^2} + \frac{2y^3}{G^3(t - t_0)^3}\right] \quad (\text{if } t - t_0 > y/G)$$
$$Y^e = 0 \quad (\text{if } t - t_0 < y/G) \tag{2}$$

where I_B is the nucleation rate per unit area of untransformed boundary.

The volume of the transformed phase depends on three covariant parameters, G, I_B, and O_V^B, while only two degrees of freedom exist, named k_B and k_G. In Thomas' original paper,[2] they are defined as "the rate at which the nucleated boundary area transforms", k_B, and "the rate at which the non-nucleated grains between the boundaries transform", k_G. The k_B and k_G rate constants, fully describing the nucleation and growth process in the C_3S hydration reaction, are connected to the linear growth rate, G, and to the nucleation rate I_B, by means of the following mathematical relationships:

$$k_B = (I_B {O_V}^B)^{1/4} G^{3/4} \tag{3}$$

$$k_G = {O_V}^B G \tag{4}$$

To achieve a numerically solvable equation, a change of variable from $y = Gt$ to $z = y/G$ is performed:[5]

$$Y^e = \frac{\pi}{3}\frac{{k_B}^4}{k_G}(t - t_0)^3 \left[1 - \frac{3z^2}{(t - t_0)^2} + \frac{2z^3}{(t - t_0)^3)}\right] \quad (\text{if } t - t_0 > z) \tag{5}$$

and hence:

$$X = 1 - \exp\left[-2k_G \int_0^{(t-t_0)} (1 - \exp(-Y^e))\, dz\right] \tag{6}$$

Equations 5 and 6 can now be solved, and the parameters k_B and k_G are directly accessed by the fitting procedure described.

By means of the DSC method, the unreacted water present in the system at each time throughout the hydration process is measured by integrating the melting peak and is expressed as the free water index (FWI) parameter.[13,14] Thus, in the DSC case, the monitoring of the disappearance of water gives direct access to the progress of the overall hydration.

The FWI versus time can be directly fitted using the generalized BNGM by explicitly introducing FWI into eq 6 as already reported in a previous study:[5]

$$FWI(t < t_d) = FWI_d + (1 - FWI_d) \times \exp\left[-2k_G \int_0^{(t-t_0)} (1 - \exp(-Y^e))dz\right] \tag{7}$$

where the parameter FWI_d is the fraction of unreacted water still present at the beginning of the diffusional period, which starts at time t_d. It is important to remember that the BNGM model is valid and can be applied only if $t < t_d$, while for $t > t_d$ a diffusion-limited approach must be adopted.

The fitting of the time evolution of the FWI using eqs 7 and 5 returns four independent parameters: k_B, k_G, FWI_d, and t_0. The values of the linear growth rate, G, and of the nucleation rate, I_B, can be then calculated by eq 3 using k_B, k_G, and O_V^B. The latter parameter, O_V^B, is 0.98 μm^{-1}, that is, the surface area of the dry powder (0.65 m^2/g, BET) scaled by the volume occupied by the hydration products after complete hydration (0.662 cm^3/g), as reported elsewhere.[5]

dx.doi.org/10.1021/jp209156n | J. Phys. Chem. C 2012, 116, 10887−10895

When the reaction time exceeds t_d, the well-known diffusion-limited description can be used to depict the hydration kinetics. At this stage, the hydration reaction is limited by the fact that water molecules must penetrate through the hydrated products layer to react with the dry fraction of the C_3S grains:

$$\mathrm{FWI}(t > t_d) = \left\{ \mathrm{FWI}_d^{1/3} - \frac{(2D)^2}{\langle R \rangle}(t - t_d)^{1/2} \right\}^3 \quad (8)$$

where FWI_d is the FWI at time t_d, D is the diffusional constant, and $\langle R \rangle$ is the average radius of the anhydrous C_3S grains (4.66 μm). Additional fitting parameters are t_d and D.

The modified BNGM equations combined with the diffusion-limited model have been implemented and numerically solved in Igor Pro, version 6.2.

RESULTS

Figure 2 shows the hydration kinetics along with the fitting curves for the pure C_3S and C_3S in the presence of PCEs. The hydration kinetics of the very same pastes have been investigated using IC at one temperature to confirm the results obtained using DSC (see the Supporting Information). Table 2 summarizes the fitting parameters obtained by means of the generalized BNGM and by the diffusion limited description. At first glance, it is evident that the main effect of the polymers is a delay in the beginning of the acceleration step, which corresponds to an extended lapse of time in which the FWI value remains fixed to unity because the water is not consumed in the formation of the hydrated phases. In the presence of superplasticizers, the kinetic curves can only be fitted by explicitly introducing an induction time, t_0, defined as the minimum delay after which the combination of k_B and k_G can account for the curve shape.

In the case where no additive is present in the C_3S paste, t_0 is always negative. Moreover, the increase in temperature leads to a slight increase in the t_0. As previously reported, a negative value of the induction time can be connected both to a faster nucleation rate per unit area (I_B) and to the fact that a certain number of nuclei is already present at the mixing time.[3] As the number of preformed nuclei is fixed and related to the prehydration of the used C_3S batch, the increase of t_0 with the temperature might be due to the fact that, as the temperature increases, the initial nucleation rate is slower as a direct consequence of the exothermic nature of the hydration reaction.

The presence of the PCEs shifts t_0 to positive values because of the inibition of the nucleation process imposed by the polymer adsorption on the C_3S grains. The magnitude of these delays varies in the following order: PCE102-2 < PCE102-6 < PCE23-2 < PCE23-6. This is consistent with the data previously reported in the literature.[22] In particular, the side chain length is a key parameter for the retardation effect, as longer side chains lead to shorter delays, decreasing the possibility for the polymer to interact with the solid phases.[22] Moreover, previous studies also showed that the esterification degree affects both the adsorption behavior (and consequently the paste workability) and the length of the initial "dormant" period: polymers with low side chain densities, that is, higher charge density on the PCE backbone, adsorb in a larger extent leading to a more pronounced retardation.[23] Consistently, the adsorption of the polymer with high side chain density and high side chain length, PCE102-2, is reported to be almost zero both on C_3S and on C−S−H.[21] In agreement with these results, a very short induction time is needed to fit the experimental data in the case of PCE102-2 addition.

Significantly, the presence of PCEs inverts the trend of t_0 versus temperature with respect to the pure C_3S paste. Most of the PCE-containing samples show a shorter t_0 as the temperature increases. This is due to the fact that the efficiency in the nucleation inibition caused by PCEs decreases as the temperature passes from 10 to 40 °C.

The column Δt_{BNG} in Table 2 reports the $t_D - t_0$ values, that is, the duration of the nucleation and growth period for each case. It is interesting to note that in the presence of PCE102-2, PCE102-6, and PCE23-2, at the same temperature, the Δt_{BNG} values are very similar and do not depend on t_0. In the presence of PCE23-6, Δt_{BNG} almost doubles that for the pure C_3S hydration. It is worth noting that the Δt_{BNG} values obtained for the PCE-containing samples are almost always longer than those obtained for the pure C_3S sample.

k_B and k_G Constants. Upon addition of PCEs, the k_B constant always decreases with respect to the pure water case. In particular, in the presence of PCE23-6, the monotonic behavior of k_B with the temperature is lost, and a maximum is found at 30 °C. Furthermore, the effect on k_G is different for each additive: PCE102-2 tends to increase k_G, PCE102-6 has a little effect on k_G, PCE23-2 tends to decrease k_G, and PCE23-6 does not show a monotonic trend for the effect of temperature on k_G, showing increased values at low temperatures and decreased k_G values at high temperatures, with respect to the pure water case. To associate the specific changes of k_G to the PCE molecular architecture, the results can be generally described as follows: the PCE23-X series tends to reduce k_G at higher temperatures, relative to the pure water case, while the PCS102-X series generally increases the k_G value (apart from PCE102-6 at 40 °C, where the value equals the one of the pure water case). These trends are strictly linked to those of the linear growth rate, G, as described later.

The k_B/k_G ratio determines the type of kinetic behavior that will be observed in the chosen experimental conditions. Three different scenarios can be drawn:

(1) $k_B/k_G \gg 1$, when the boundary area per unit volume O_V^B is small and I_B/G (nucleation rate/linear growth rate ratio) is large: in this case, the boundary area is densely populated with nuclei, and the whole transformation occurs in the very early stages of the process.

(2) $k_B/k_G \ll 1$: If O_V^B is large and I_B/G is small, the nuclei are sparsely distributed on the internal boundaries. In this case, the conditions approach the "spatially random nucleation" required for the Avrami−Erove'ev equation, holding the following relationship:

$$k_{avr} = (\pi/3)^{1/4} k_B \quad (9)$$

(3) $k_B/k_G \approx 1$: None of the previous limiting conditions are satisfied.

Pure C_3S paste matches the third case, the value of k_B/k_G being 1 (within 1 standard deviation) at all temperatures. The k_B/k_G ratios obtained for the pastes with PCE102-X superplasticizers are always less than 1, indicating a sparser presence of nucleation sites. For this PCE series, the ratios remain almost constant, around 0.7 ± 1 standard deviation, in the entire temperature range (apart from PCE102-2 at 40 °C, which is lower). For PCE23-X polymers, instead, the A−E conditions are closer at low temperatures, with the k_B/k_G being lower than 1, while at higher temperatures k_B/k_G is closer to unity.

dx.doi.org/10.1021/jp209156n | J. Phys. Chem. C 2012, 116, 10887−10895

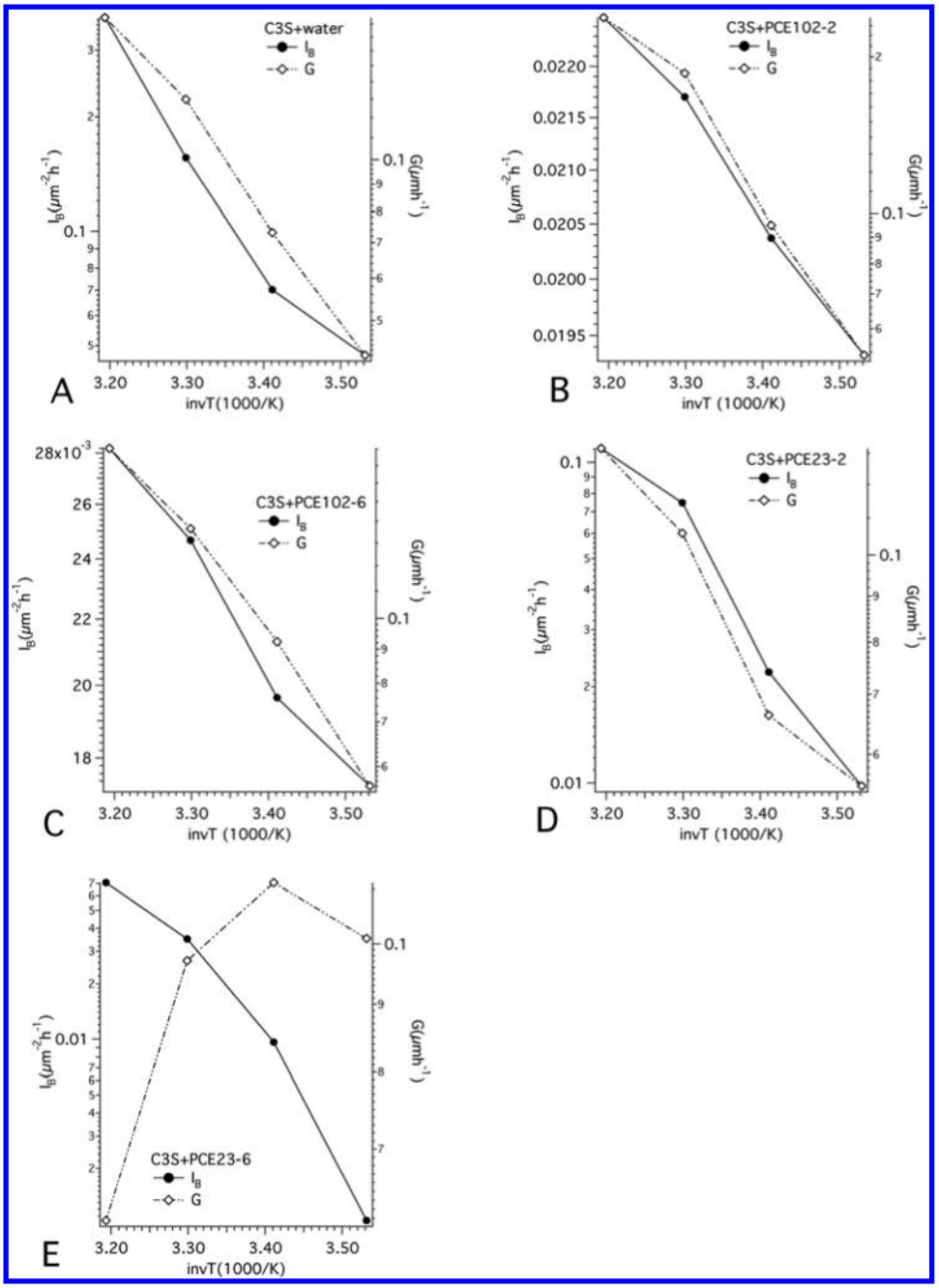

Figure 3. Nucleation rate, I_B, and linear growth rate, G, calculated from the generalized BNGM fits of (A) C_3S in pure water, (B) C_3S+PCE102-2, (C) C_3S+PCE102-6, (D) C_3S+PCE23-2, and (E) C_3S+PCE23-6.

***I_B* and *G*.** Figure 3 shows the trends of the nucleation and linear growth rates obtained for the investigated systems by means of eqs 3 and 4, and Table 3 reports the calculated values. In all cases, the addition of PCE reduces the nucleation rates, I_B, following the trend PCE23-6 > PCE23-2 ≈ PCE102-6 > PCE102-2 ≈ H_2O. Considering the linear growth rates, G, the order of magnitude remains approximately unaltered. It is worth noting that for PCE23-6 only, the temperature dependence of G is not monotone, and this aspect can be at the origin of the super-Arrhenius behavior found in the case of k_G and k_B values.

Temperature Dependence of Rate Constants: Activation Energies. The temperature dependence of the reaction rates follows the well-known Arrhenius equation:

$$k(T) = A\exp\left(-\frac{E_a}{RT}\right) \tag{10}$$

This is considered an almost general behavior, at least in the common temperature range of the biosphere, because the temperature dependences included in the A factor (predicted, for example, in the transition state or collision theories, or due to generic entropic contributions) are usually weak with respect to the exponential dependence. Actually, these unspecified factors become sometimes relevant to determine important deviations from the linearity of the Arrhenius plots (see later description on the effect of PCE23-6).

The Arrhenius plots of both k_G and k_B are linear in the range 10−40 °C for the C_3S/H_2O paste (see Figure 4 A). In particular, the slopes of the linear fits give activation energies of

dx.doi.org/10.1021/jp209156n | J. Phys. Chem. C 2012, 116, 10887−10895

Table 3. Nucleation Rate, I_B, and Linear Growth Rate, G, Determined from the Generalized BNGM Fitting of Hydration Kinetics as a Function of the Polymer Addition and Temperature

T (°C)	I_B (μm^{-2} h^{-1})	G ($\mu m h^{-1}$)
H_2O		
10	0.047(7)	0.043(2)
20	0.07(6)	0.07(2)
30	0.16(3)	0.130(3)
40	0.4(2)	0.18(3)
PCE102-2		
10	0.019(5)	0.053(4)
20	0.020(1)	0.0948(9)
30	0.022(7)	0.19(2)
40	0.022(1)	0.238(2)
PCE102-6		
10	0.017(5)	0.056(5)
20	0.020(3)	0.092(3)
30	0.03(1)	0.14(1)
40	0.03(2)	0.18(2)
PCE23-2		
10	0.010(4)	0.055(4)
20	0.022(1)	0.066(1)
30	0.07(3)	0.11(3)
40	0.110(2)	0.132(2)
PCE23-6		
10	0.001(9)	0.10(1)
20	0.010(2)	0.111(2)
30	0.03(2)	0.10(2)
40	0.071(2)	0.062(2)

34.7 and 39.4 kJ/mol for k_G and k_B, respectively. These values are very similar to those previously reported for pure C_3S hydration, where t_0 was not explicitly considered.[2,5]

Similarly, when PCE102-2, PCE102-6, or PCE23-2 is added to the mix, the Arrhenius plots of k_B and k_G have linear trends (see Figure 4B–D and Table 4). The activation energies obtained for these systems are lower than those calculated for C_3S hydrated with pure water (except for the PCE102-2 in the case of k_G). For this reason, the presence of the PCEs would reduce the influence of T with respect to the nucleation and the growth processes, mitigating the formation of inhomogeneities in the hydrated phases, and the thermal contraction, thus reducing unwanted cracking.[29] As expected, the PCE102-2, which shows a lower propensity to adsorb on the C_3S grains than the others PCE under investigation,[21] exploits a small effect on both kinetic processes, while the decrease in the degree of substitution (PCE102-6) or the decrease in the branch length (PCE23-2) results in increased setting delays and superplasticizing skills.

In the PCE23-6 case the reaction cannot be described as a single thermally activated process: Arrhenius plots (Figure 4E) clearly show a parabolic (convex) trend. Such a deviation from the linearity has been previously described as super-Arrhenius behavior,[30] indicated by an increasing apparent activation energy with decreasing temperature (note that, from now on, the activation energies will be referred to as apparent because they have been extracted from a super-Arrhenius trend):

$$E_a(T) = \frac{-\partial \ln k}{\partial\left(\frac{1}{RT}\right)} \tag{11}$$

Figure 5 shows the linearity of the activation energies versus $1/T$ plots, in the cases of the hydration process of tricalcium silicate with PCE23-6 polymer.

The PCE23-6 completely changes the nature of the hydration reaction and its response to the temperature. In particular, as T increases, the apparent activation energy passes from positive to negative values, and the "thermal activated" behavior is recovered only at low T (10–20 °C). It is important to stress that negative values for activation energy are unphysical, because they clash with the definition ("activation" cannot be negative).

Results shown in Figures 4E and 5 clearly indicate that in the case of additive PCE23-6 the adopted model fails to provide a physical description of the experimental data. This deviation might be due to both changes in the nature of the hydrated products or differences in the kinetic mechanisms. In the second scenario, it is possible that the nonmonotonic behavior is a result of the coexistence of diffusional and nucleation-and-growth processes, even considering the huge period of time involved in the hydration reaction. Further studies are needed to ascertain this point.

Inspection of Figure 4B and C reveals deviations from linearity at 40 °C for PCE102-2 and PCE102-6. A similar behavior has been already reported previously.[2] We do not consider these deviations here, as they are small.

***D*, Diffusional Constant.** The last part of all of the curves was fitted with a diffusional model. The parameter D extracted from these fitting gives information on the ease of the soluble molecules (mainly water) to diffuse through the hydrated phases' dense matrix formed after the acceleration period. The results, which are reported in the last column of Table 2 together with standard deviation, do not show any trend with the temperature, indicating that the two contributions affecting diffusion (the thermal activation of diffusional processes and the higher density of the gel phase at higher temperatures) compensate each other.

CONCLUSIONS

The kinetics of tricalcium silicate hydration in the presence of a series of comb-shaped PCE superplasticizers with controlled chemical architecture have been followed by DSC and characterized using the generalized BNGM. These polymers have been found to delay the beginning of the nucleation and growth process. The generalized BNGM introduces the induction time, t_0, to explicitly consider this delay. In accordance with previous literature, decreasing the length of the polyethylene oxide side chains increases the induction time, and for this reason induction times are longer for the PCE23-X series than for the PCE102-X. Furthermore, the induction times increase as the degree of substitution of the polycarboxylic backbone decreases; that is, PCEX-6 polymers (n:m = 6:1, one esterified carboxylic group per six unsubstituted carboxylic groups) show longer t_0 than do those of PCEX-2 (n:m = 2:1, one esterified carboxylic group per two unsubstituted carboxylic groups).

The presence of PCEs in the mix nearly always increases the total duration of the nucleation and growth period with respect to the pure water case.

The modified BNGM successfully describes the time-evolution of the free water index in the nucleation and growth period through the rate constants k_G and k_B, which quantify the effect of the polymers on the kinetics of hydration. The overall effect of PCE addition is a decrease of k_B with respect to the

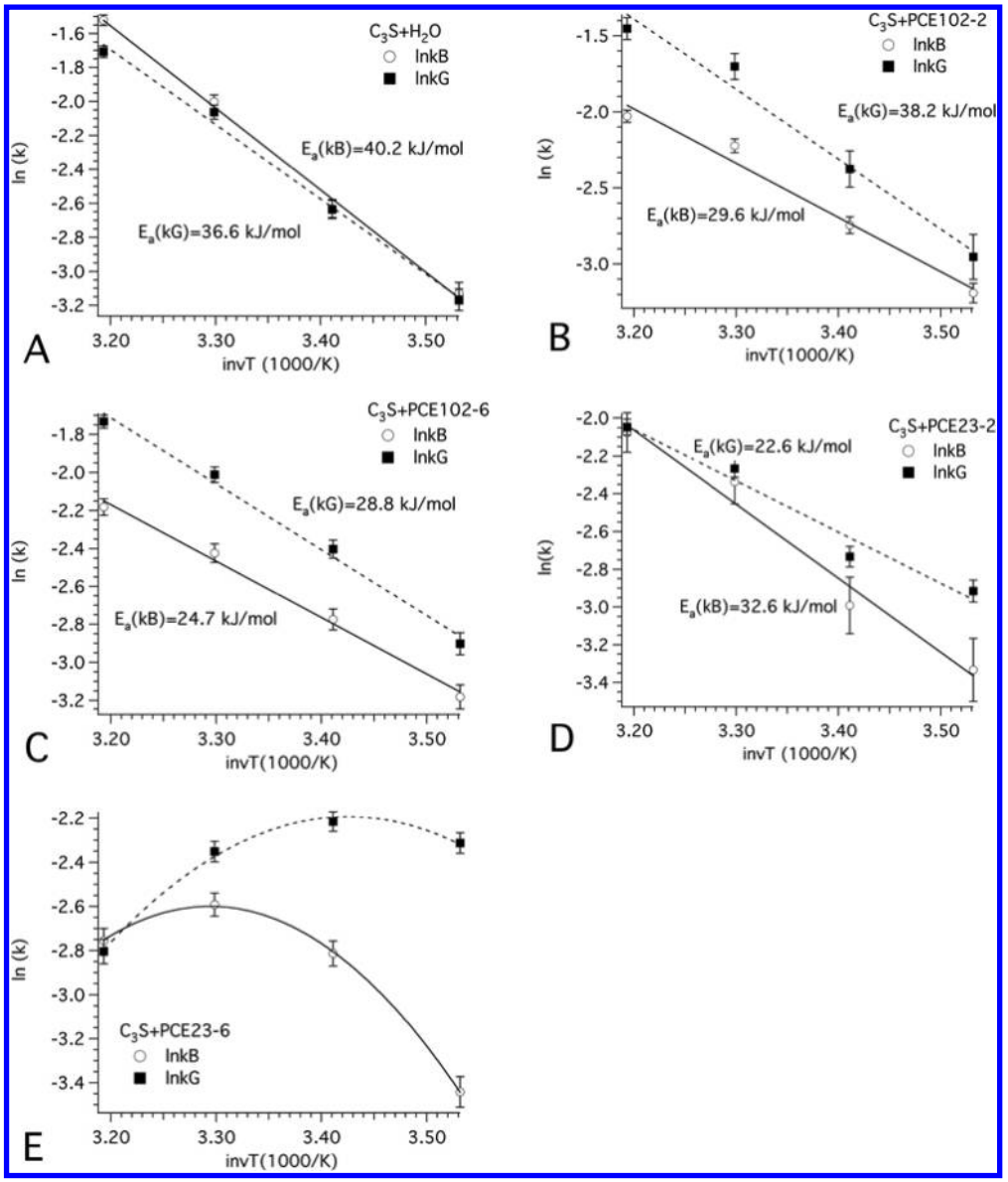

Figure 4. Arrhenius plots of k_B and k_G rate constants obtained from the generalized BNGM of C_3S hydration kinetics (A) in pure water, (B) with PCE102-2, (C) with PCE102-6, (D) with PCE23-2, and (E) with PCE23-6.

Table 4. Effect of the PCE Superplasticizers on the Activation Energies Associated with the Rate Constants, k_B and k_G

	$E_a(k_B)$, kJ/mol	$E_a(k_G)$, kJ/mol
H_2O	40.2(2)	36.6(2)
PCE102-2	29.6(4)	38.2(5)
PCE102-6	24.7(2)	28.8(2)
PCE23-2	32.6(4)	22.6(3)
PCE23-6	nonlinear	nonlinear

C_3S/water case. On the other hand, the effect on k_G is more complex and can hardly be associated with specific changes in the PCE molecular architecture. As a general trend, it is worth noting that the PCE23-X series tends to reduce the linear growth rate G (and therefore k_G) at higher temperatures, relative to the pure water case, while the PCE102-X series generally increases the G value (apart from PCE102-6 at 40 °C, where G equals the value of the pure water case). The k_B/k_G ratios of the additivated pastes are mainly lower than those of

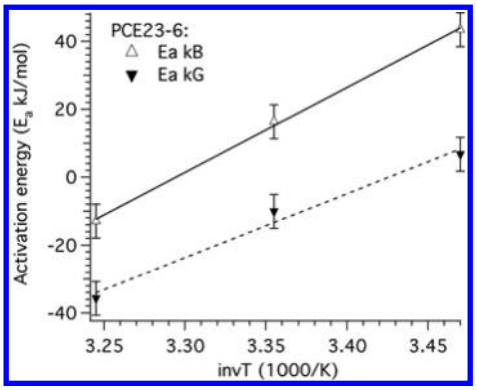

Figure 5. $1/T$ dependence of the k_B and k_G apparent activation energies for the C_3S/PCE23-6 system.

the neat case. In particular, k_B/k_G for the pastes with PCE102-X are always less than 1, indicating a sparse presence of nucleation sites. Moreover, for this series, the ratios decrease as the

dx.doi.org/10.1021/jp209156n | J. Phys. Chem. C 2012, 116, 10887−10895

temperature rises. The reverse situation is found for short side chain polymers (PCE23-X), where the k_B/k_G ratios increase with increasing temperature, and become equal to 1 at 40 °C.

The Arrhenius plot of the rate constants evidences an Arrhenius behavior in all cases except for the polymer having shorter side chains and a lower degree of substitution. In this latter case, a super-Arrhenius trend is clearly evidenced, possibly as a result of the coexistence of different mechanisms along with the nucleation-and-growth process.

■ ASSOCIATED CONTENT

Supporting Information

(a) Experimental method for isothermal calorimetry measurements. (b) Figure 1: Heat flow versus time plot, obtained by isothermal calorimetry, of C_3S pastes without and with superplasticizer. (c) Figure 2: Cumulative heat development. This material is available free of charge via the Internet at http://pubs.acs.org.

■ AUTHOR INFORMATION

Corresponding Author

*Phone: +39 055 457-3033. Fax: +39 055 457-3032. E-mail: piero.baglioni@unifi.it.

Notes

The authors declare no competing financial interest.

■ ACKNOWLEDGMENTS

We kindly thank CTG-Italcementi for providing the C_3S pure phase and for partial financial support. Dr. Stefan Becker and Dr. Joachim Pakusch (BASF AG, Ludwigshafen, Germany) are acknowledged for providing the PCE superplasticizers. Partial financial support from Ministero dell'Istruzione, Università e della Ricerca Scientifica (MIUR, grant PRIN-2008, prot. 20087K9A2J), and Consorzio Interuniversitario per lo Sviluppo dei Sistemi a Grande Interfase, CSGI, is gratefully acknowledged. We thank the referees for their positive and constructive comments that greatly improved the final version of this paper.

■ REFERENCES

(1) Taylor, H. *Cement Chemistry*; Thomas Telford Publishing: London, UK, 1997.
(2) Thomas, J. J. *J. Am. Chem. Soc.* **2007**, *90*, 3282−3288.
(3) Thomas, J. J.; Allen, A. J.; Jennings, H. M. *J. Phys. Chem. C* **2009**, *113*, 19836−19844.
(4) Peterson, V. K.; Whitten, A. E. *J. Phys. Chem. C* **2009**, *113*, 2347−2351.
(5) Ridi, F.; Fratini, E.; Luciani, P.; Winnefeld, F.; Baglioni, P. *J. Colloid Interface Sci.* **2011**, *364*, 118−124.
(6) Thomas, J. J.; Jennings, H. M.; Chen, J. *J. Phys. Chem. C* **2009**, *113*, 4327−4334.
(7) Ridi, F.; Fratini, E.; Milani, S.; Baglioni, P. *J. Phys. Chem. B* **2006**, *110*, 16326−16331.
(8) Berliner, R.; Popovici, M.; Herwig, K. W.; Berliner, M.; Jennings, H. M.; Thomas, J. J. *Cem. Concr. Res.* **1998**, *28*, 231−243.
(9) Fratini, E.; Chen, S. H.; Baglioni, P.; Bellissent-Funel, M. C. *J. Phys. Chem. B* **2002**, *106*, 158−166.
(10) Fratini, E.; Chen, S. H.; Baglioni, P.; Cook, J. C.; Copley, J. R. D. *Phys. Rev. E* **2002**, *65*, 010201.
(11) Faraone, A.; Fratini, E.; Baglioni, P.; Chen, S. H. *J. Chem. Phys.* **2004**, *121*, 3212−3220.
(12) Peterson, V. K.; Neumann, D. A.; Livingston, R. A. *J. Phys. Chem. B* **2005**, *109*, 14449−14453.
(13) Damasceni, A.; Dei, L.; Fratini, E.; Ridi, F.; Chen, S. H.; Baglioni, P. *J. Phys. Chem. B* **2002**, *106*, 11572−11578.
(14) Ridi, F.; Dei, L.; Fratini, E.; Chen, S. H.; Baglioni, P. *J. Phys. Chem. B* **2003**, *107*, 1056−1061.
(15) Ridi, F.; Fratini, E.; Mannelli, F.; Baglioni, P. *J. Phys. Chem. B* **2005**, *109*, 14727−14734.
(16) Yoshioka, K.; Tazawa, E.; Kawai, K.; Enohata, T. *Cem. Concr. Res.* **2002**, *32*, 1507−1513.
(17) Zingg, A.; Holzer, L.; Kaech, A.; Winnefeld, F.; Pakusch, J.; Becker, S.; Gauckler, L. *Cem. Concr. Res.* **2008**, *38*, 522−529.
(18) Flatt, R. J.; Houst, Y. F. *Cem. Concr. Res.* **2001**, *31*, 1169−1176.
(19) Yamada, K.; Ogawa, S.; Hanehara, S. *Cem. Concr. Res.* **2001**, *31*, 375−383.
(20) Prince, W.; Espagne, A.; Aitcin, P. C. *Cem. Concr. Res.* **2003**, *33*, 635−641.
(21) Zingg, A.; Winnefeld, F.; Holzer, L.; Pakusch, J.; Becker, S.; Gauckler, L. *J. Colloid Interface Sci.* **2008**, *323*, 301−312.
(22) Zingg, A.; Winnefeld, F.; Holzer, L.; Pakusch, J.; Becker, S.; Figi, R.; Gauckler, L. *Cem. Concr. Comp.* **2009**, *31*, 153−162.
(23) Winnefeld, F.; Becker, S.; Pakusch, J.; Goetz, T. *Cem. Concr. Comp.* **2007**, *29*, 251−262.
(24) Yamada, K.; Takahashi, T.; Hanehara, S.; Matsuhisa, M. *Cem. Concr. Res.* **2000**, *30*, 197−207.
(25) Sakai, E.; Yamada, K.; Ohta, A. *J. Adv. Concr. Technol.* **2003**, *1*, 16−25.
(26) Kirby, G. H.; Lewis, J. A. *J. Am. Ceram. Soc.* **2004**, *87*, 1643−1652.
(27) Li, C. Z.; Feng, N. Q.; Li, Y. D.; Chen, R. J. *Cem. Concr. Res.* **2005**, *35*, 867−873.
(28) Cahn, J. *Acta Metall.* **1956**, *4*, 449−459.
(29) Hewlett, P. C. *Lea's Chemistry of Cement and Concrete*; Arnold: London, UK, 1998.
(30) Nishiyama, M.; Kleijn, S.; Aquilanti, V.; Kasai, T. *Chem. Phys. Lett.* **2009**, *482*, 325−329.